Supplemental Data
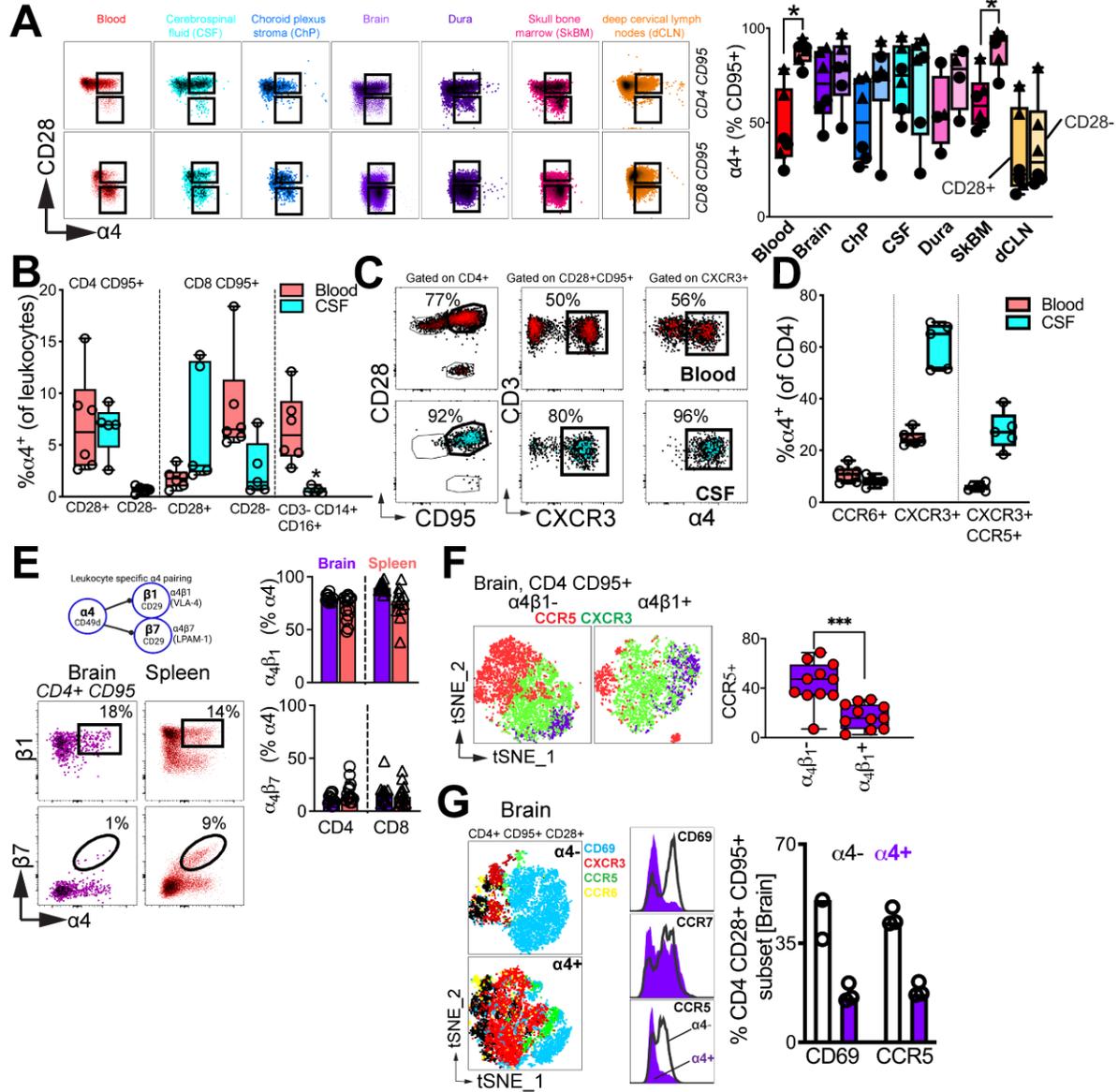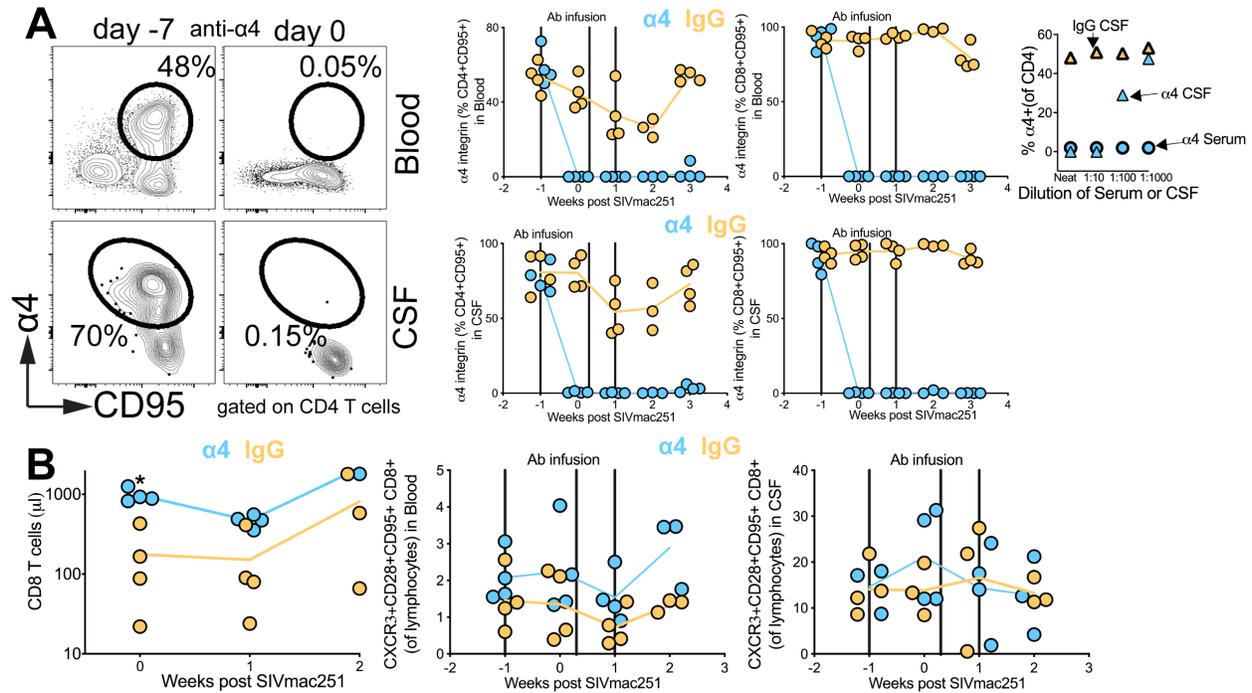

Supplementary Figure 1. Integrin and chemokine receptor profiling of α4⁺ T cells across CNS and systemic compartments. (A) α4 integrin expression in CD28⁻ and CD28⁺ T cell subsets (n=7 animals across 6 tissues) across indicated tissues; cells are color-coded by tissue of origin in both flow plots and box plots. (**B**) Frequencies of α4⁺ CD28⁺ and CD28⁻ CD4 and CD8 T cells compared with α4⁺ monocytes in blood and cerebrospinal fluid (CSF). (**C**) Representative flow cytometry gating strategy for CD28⁺ CD95⁺ T cells in blood (red, top) and CSF (blue, bottom), with CXCR3 expression and corresponding α4 integrin expression shown on the CXCR3⁺ subset. (**D**) Distribution of CXCR3⁺ (T$_h$1) and CCR6⁺ (T$_h$17) subsets and target T$_h$1 cells (CCR5⁺ CXCR3⁺) within α4⁺ CD4 T cells in blood and CSF. (**E**) Co-expression of β1 and β7 integrin chains on α4⁺ T cells in brain and spleen. (**F**) Chemokine receptor expression profiles of α4β1⁻ and α4β1⁺ CD4 T cells (n=11) in the brain. (**G**) Expression of CD69, CCR7, and CCR5 on α4⁻ and α4⁺ CD4 T cells in the brain. *p < 0.05, two-tailed t-test **(A)**; ***p < 0.001, two-tailed t-test **(F)**. ChP, choroid plexus stroma; SkBM, skull bone marrow; dCLN, deep cervical lymph nodes.

Supplementary Figure 2. α4 integrin blockade and T cell subset kinetics in blood and cerebrospinal fluid. (A) α4 integrin receptor occupancy analysis demonstrating sustained blockade on T cells in blood and cerebrospinal fluid (CSF) following α4 antibody administration. Inset shows ex vivo receptor occupancy assay, in which pre-infusion PBMCs were incubated with serum (circles) or CSF (triangles) from α4-treated animals, resulting in loss of detectable surface α4 expression, which was recovered by dilution of CSF but not serum. CSF from IgG-treated animal shown as control. **(B)** Longitudinal frequencies of total CD8 T cells and CXCR3+ CD8 T cell subsets in blood and CSF over time following α4 blockade. *p < 0.05, one-tailed unpaired Mann–Whitney test; n = 4 per group.
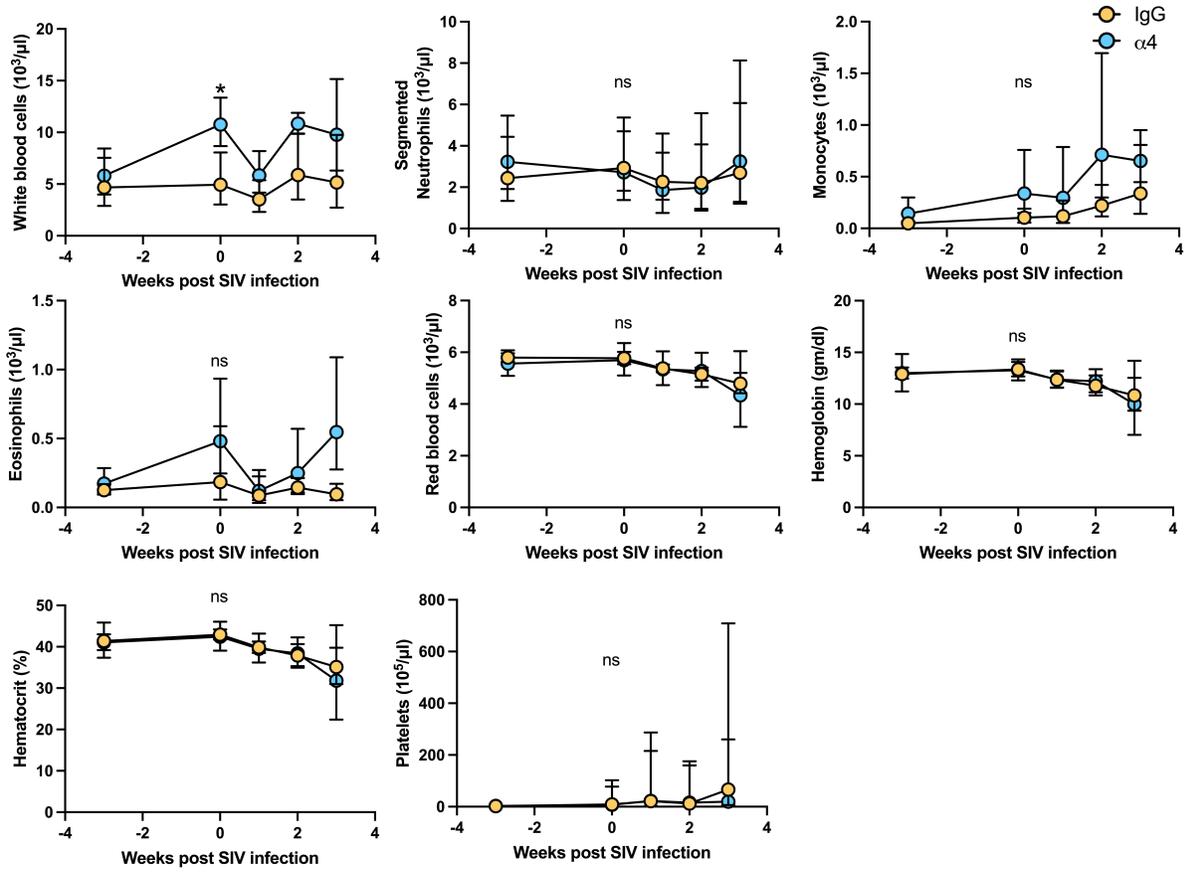
Supplementary Figure 3. α4 integrin blockade does not alter innate immune cell frequencies or hematologic parameters. Longitudinal measurements of circulating monocytes, neutrophils, eosinophils, red blood cells, hemoglobin, hematocrit, and platelets in α4-treated and IgG-treated animals. Data are shown as geometric mean with standard deviation. n = 4 animals per group.
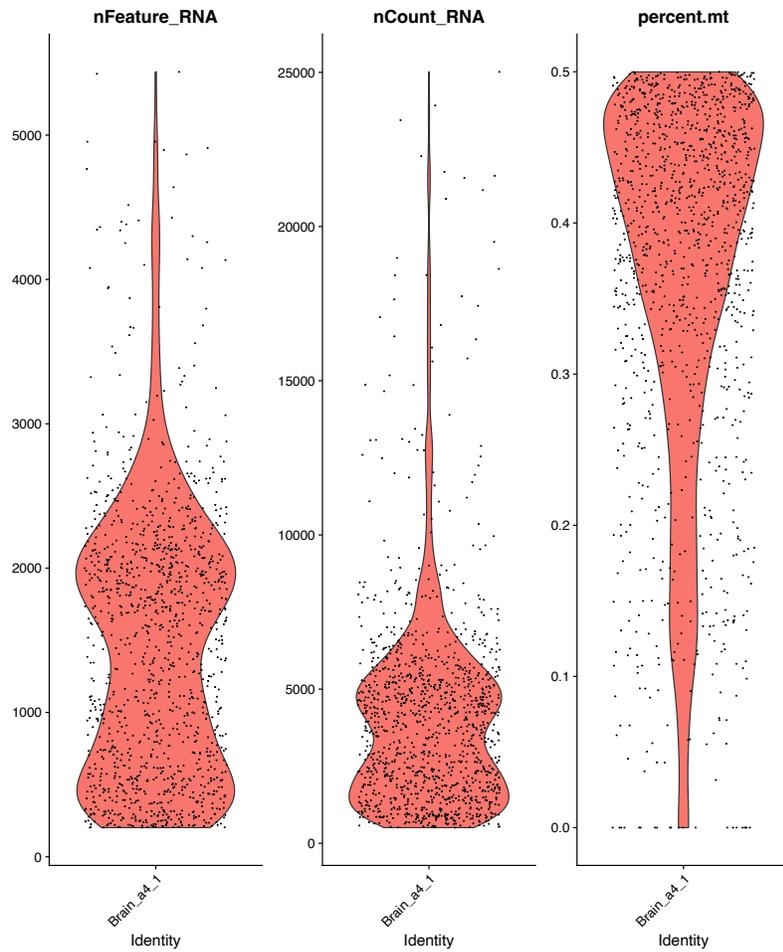
Supplementary Figure 4A. Single-cell RNA sequencing quality control metrics for a representative brain sample (α4 replicate A4_1, n = 4 total samples). Violin plots display the distribution of detected genes per cell (nFeature_RNA), total transcript counts per cell (nCount_RNA), and the proportion of mitochondrial transcripts (percent.mt) across CD45+ brain immune cells from one α4-treated animal (Brain A4_1). Each point represents an individual cell. These metrics were used to assess data quality and to exclude low-quality cells prior to downstream clustering and differential expression analyses.
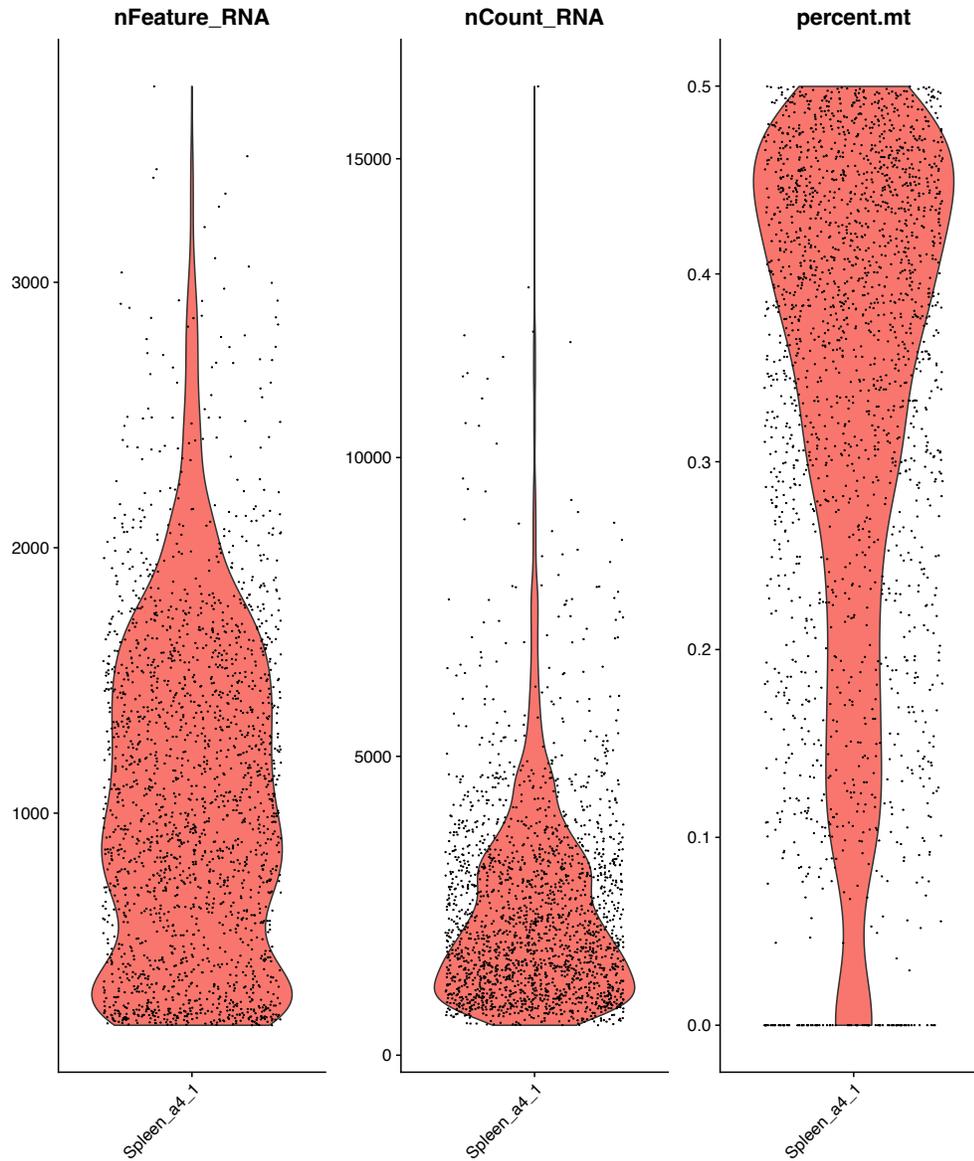
Supplementary Figure 4B. Single-cell RNA sequencing quality control metrics for a representative spleen sample (α4 replicate A4_1, n = 4 total samples). Violin plots display the distribution of detected genes per cell (nFeature_RNA), total transcript counts per cell (nCount_RNA), and the proportion of mitochondrial transcripts (percent.mt) across CD45^{+} spleen immune cells from one α4-treated animal (Spleen A4_1). Each point represents an individual cell. These metrics were used to assess data quality and to exclude low-quality cells prior to downstream clustering and differential expression analyses.
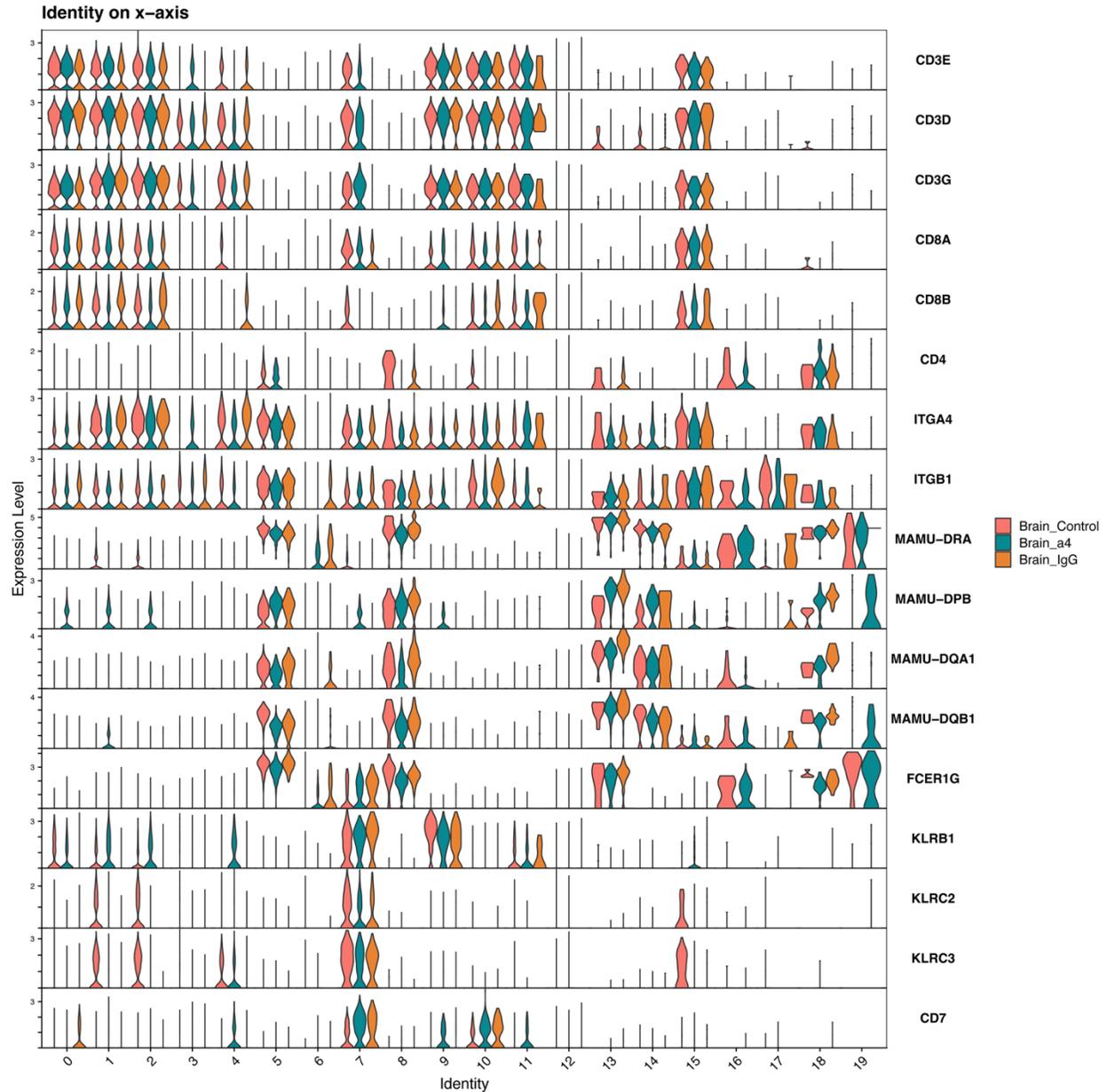
Supplementary Figure 5. Distribution of *ITGA4* expression across brain immune subclusters in control, α4-treated, and IgG-treated animals. *ITGA4* gene expression is shown across 20 annotated brain immune subclusters, displayed separately for control (n = 2), IgG-treated (n = 4), and α4-treated (n = 4) animals (see Figure 2C for consolidated expression across all conditions). Control data were previously published (Ref #3).
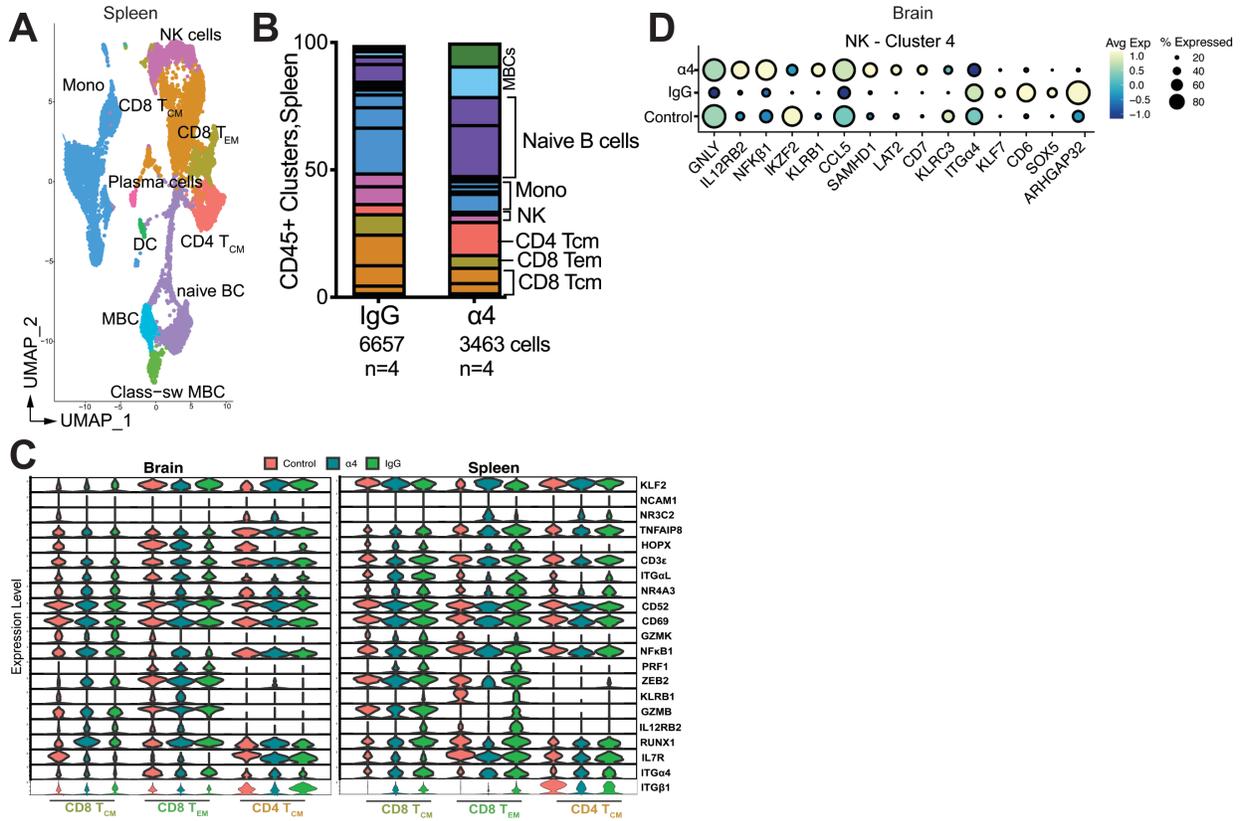
Supplementary Figure 6. Distribution of *ITGA4* expression across spleen immune populations. (**A–C**) UMAP visualizations of spleen immune populations, including B cell clusters absent from the brain dataset, shown in control (n = 2), IgG-treated (n = 4), and α4-treated (n = 4) animals. (**D**) Dot plot showing transcriptional features of the NK cell cluster in the brain. Control data were previously published (Ref #3).
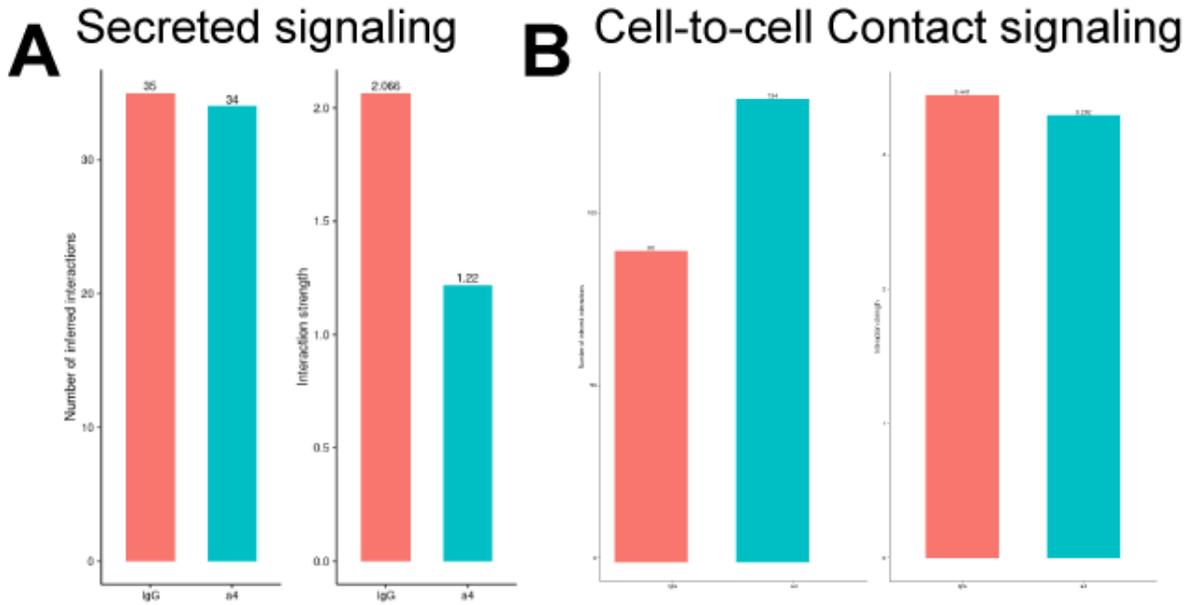
Supplementary Figure 7. Inferred secreted and contact-mediated signaling under α4 integrin blockade. (A) CellChat analysis showing reduced strength, but not number, of predicted secreted signaling interactions following α4 blockade. **(B)** In contrast, contact-mediated signaling exhibits an increased number of interactions under blockade, while overall interaction strength remains comparable between groups. n = 3 per group.
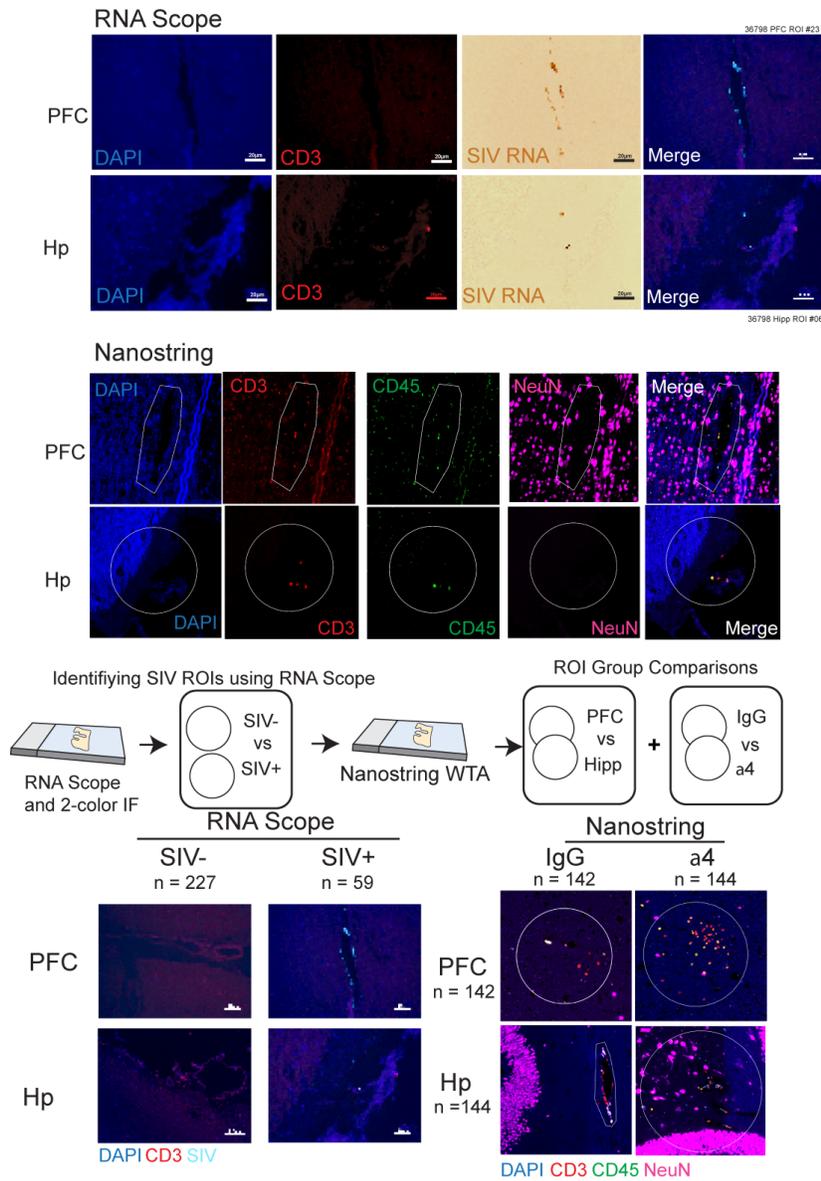
Supplementary Figure 8. Spatial ROI selection and sample overview for Nanostring transcriptomic analysis. Representative tissue sections showing SIV RNA[+] and SIV[−] regions identified by RNAscope in situ hybridization, which were used to guide region of interest selection for downstream NanoString whole transcriptome analysis (WTA). n = 3 per group, Scale bar: 20μm.
The RNAscope image in the S8 top panel is reused in the S8 lower left panel (SIV[+]/HP). All analyses and quantification were performed on independent biological replicates.
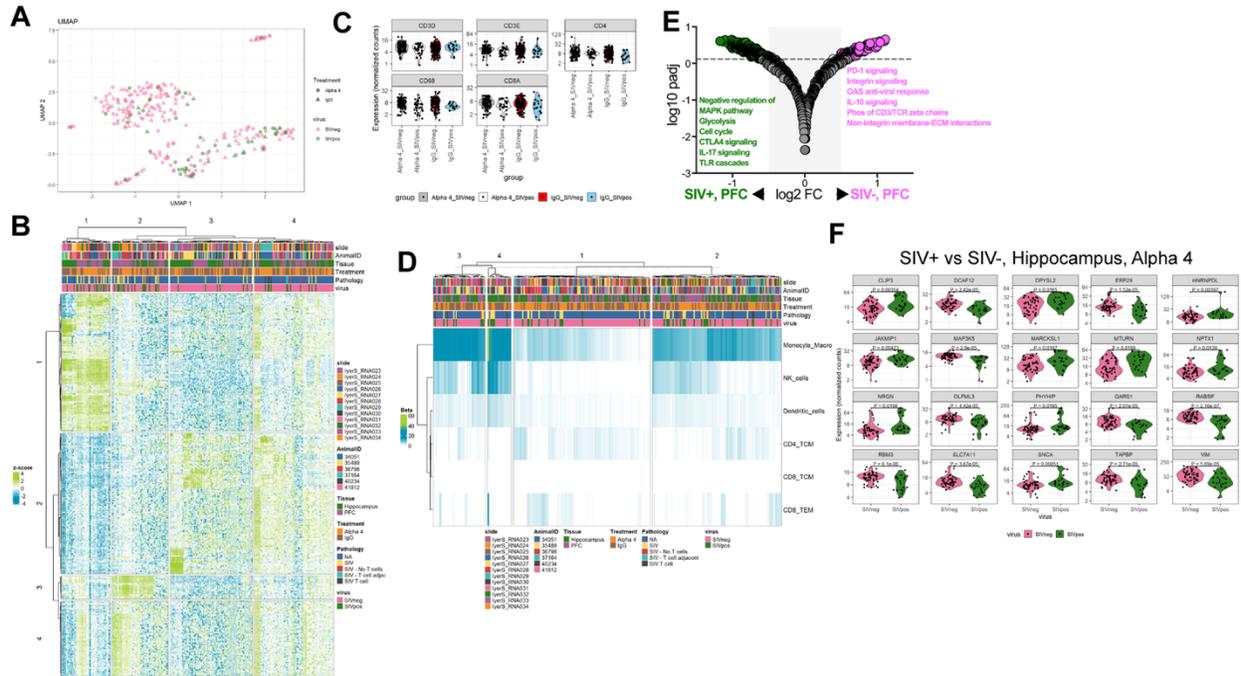
Supplementary Figure 9. SIV RNA status drives spatial clustering and immune cell localization.
(A–B) Dimensionality reduction of NanoString whole transcriptome data showing region of interest clustering primarily by SIV RNA status. **(C)** Spatial expression of immune marker transcripts (CD3, CD4, CD8, CD68) confirming localization of T cell and myeloid populations across regions of interest. **(D)** Composition of the sc-RNA-seq-derived reference used for spatial deconvolution, showing marker genes defining CD4 T cell, CD8 T cell, NK cell, dendritic cell, and myeloid clusters used to estimate cell type proportions in spatial segments. **(E)** Volcano plot displaying the distribution of differentially expressed genes with adjusted P values. **(F)** Violin plots showing differences in gene expression across SIV- versus SIV+ hippocampal regions in α4-treated animals. n = 3 per group.
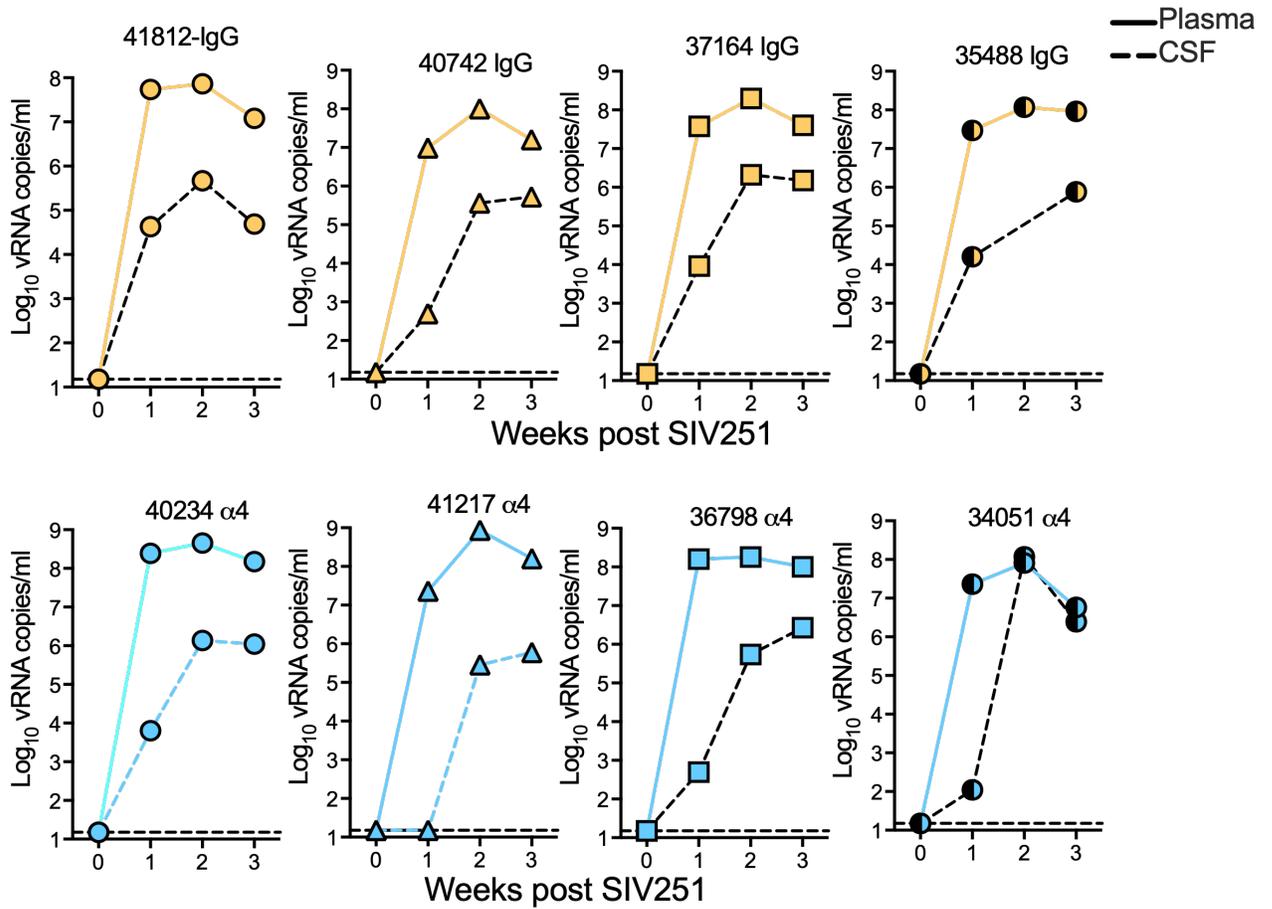
Supplementary Figure 10. Individual viral kinetics in plasma and cerebrospinal fluid by treatment group. Longitudinal plasma (solid line) and cerebrospinal fluid (CSF, dashed line) viral(v) RNA levels for individual animals from weeks 1 to 3 post-infection in α4-treated and IgG-treated groups.
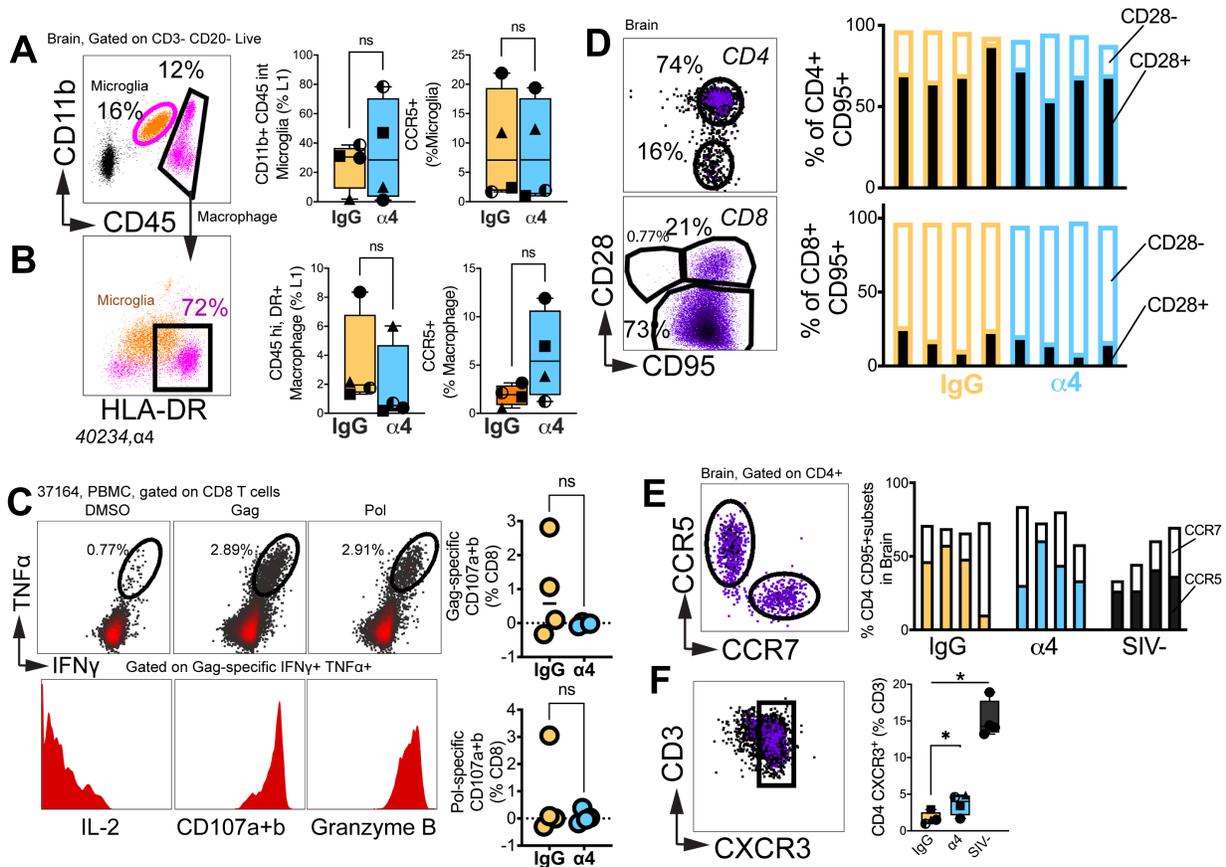
Supplementary Figure 11. Myeloid and T cell subset characterization in brain tissue following α4 integrin blockade in macaques. (**A–B**) Quantification of microglia and macrophages in brain tissue from α4-treated and IgG-treated animals, showing no significant differences between groups. (**C**) Flow plot shows SIV-specific T cell responses to Gag and Pol peptides by ICS in blood; histograms show expression of IL-2 and cytolytic molecules on Gag-specific IFNγ+ TNFα+ CD8 T cells; scatter plots show frequencies of DMSO-subtracted Gag-and Pol-specific CD8 T cells across groups. (**D**) Expression profiles of CD28+ and CD28− CD4 T cell subsets in the brain. (**E**) Expression of chemokine receptors CCR5 and CCR7 on brain-infiltrating CD4 T cells. (**F**) Frequencies of CXCR3+ CD4 T cells within the brain parenchyma, showing reduced integrin-expressing subsets following α4 blockade. *p < 0.05, one-tailed unpaired Mann–Whitney test; n = 4 per group.
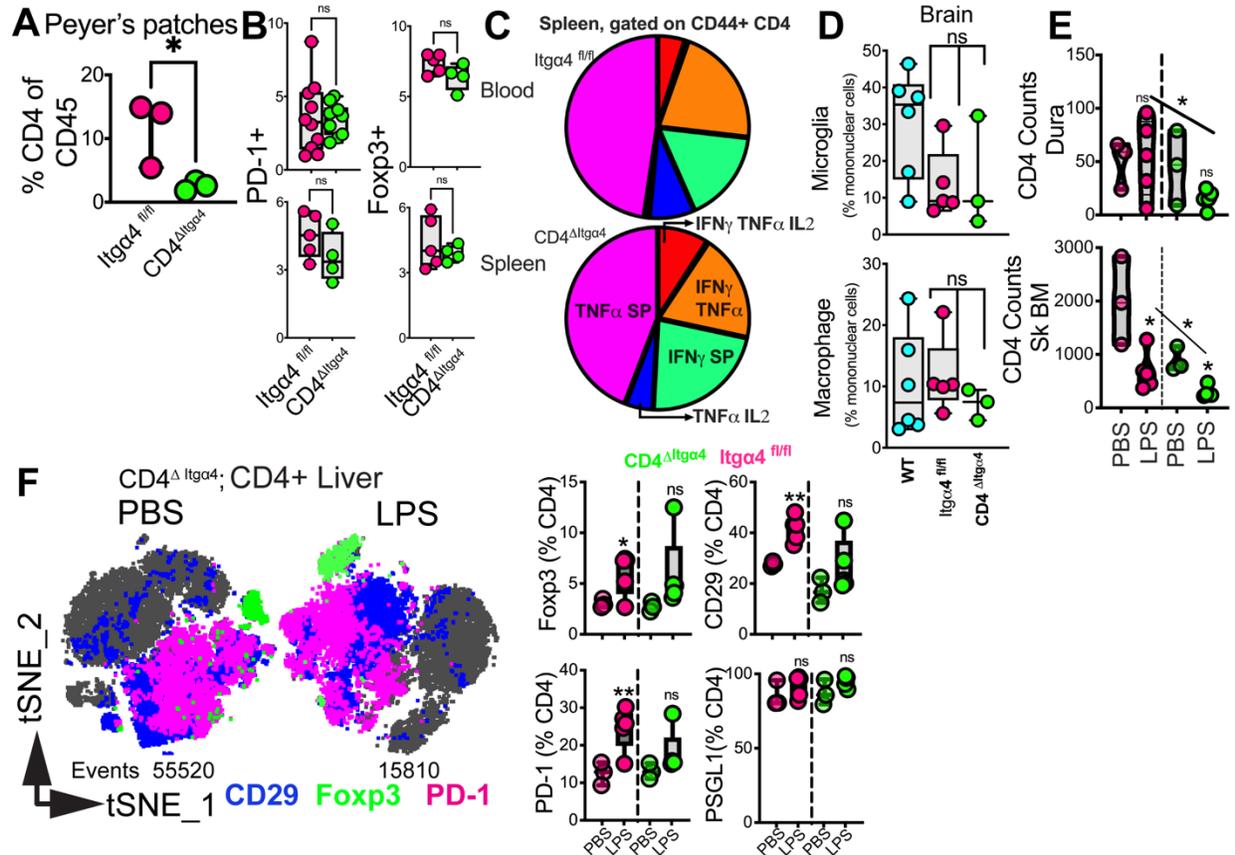
Supplementary Figure 12. Effects of α4 integrin deletion on CD4 T cell distribution and phenotype across tissues. (A) Reduced frequencies of CD4 T cells in Peyer's patches of CD4^{ΔItgα4} mice. (**B**) PD-1 and Foxp3 expression in circulating and splenic CD4 T cells across genotypes. (**C**) Boolean analysis of cytokine-producing CD44$^+$ CD4 T cells in the spleen following PMA and ionomycin stimulation. (**D**) Frequencies of brain-resident innate immune populations, including microglia and macrophages, across groups. (**E**) CD4 counts in dura and skull bone marrow. (**F**) Phenotypic profiling of liver CD4 T cells following LPS challenge, showing comparable activation and trafficking-associated marker expression across genotypes. Data represent 3–5 animals per group from ≥3 independent experiments.
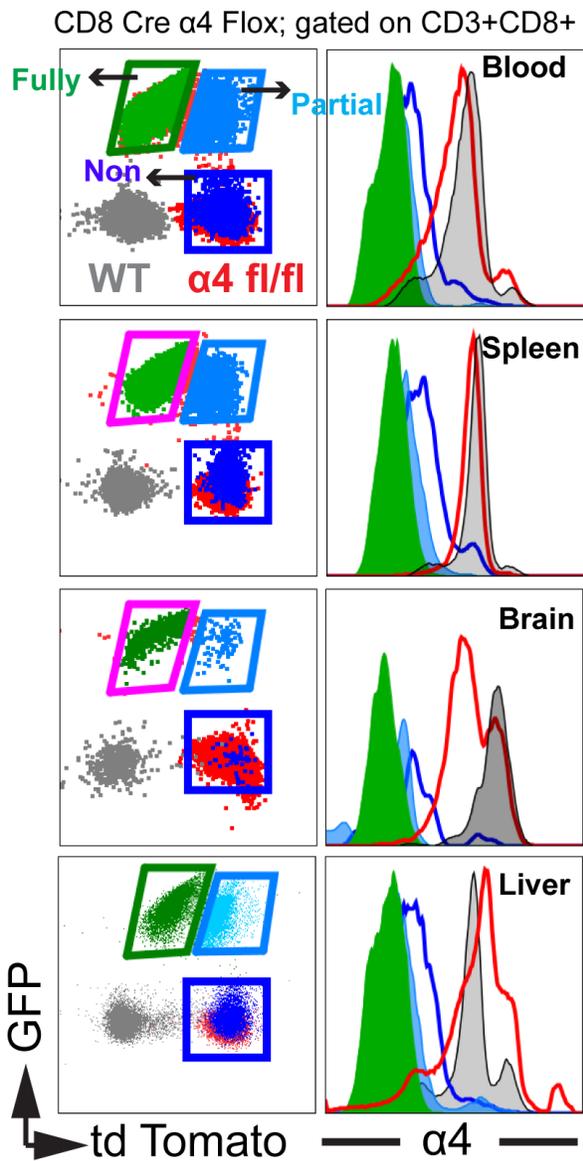
Supplementary Figure 13. Mosaic recombination of *Itgα4* in CD8^{ΔItgα4} mice. Representative flow cytometry plots illustrating fully recombined (GFP$^+$ tdTomato$^-$), partially recombined, and non-recombined CD8 T cell populations in CD8^{ΔItgα4} mice across blood, spleen, brain, and liver. Data represent 3–5 animals per group from ≥3 independent experiments.

S1 Table. Nonhuman primate cohorts.

Group	Animal ID	Sex	Age (years. months) at Nx.	Weight (kg) at Nx.	Site	Virus $(1 \times 10^4 \text{ TCID}_{50})$	IgG antibody* control (25mg/kg)	ART Regimen
α4 blockade study (n=8)	41812	F	11.02	7.30	CNPRC	SIVmac251	Anti-desipramine	-
	40742	M	12.04	12.00	CNPRC	SIVmac251	Anti-desipramine	-
	37164	F	16.01	10.83	CNPRC	SIVmac251	Anti-desipramine	-
	35488	F	17.04	10.48	CNPRC	SIVmac251	Anti-desipramine	-
	40234	F	12.11	9.34	CNPRC	SIVmac251	Anti-α4	-
	41217	F	11.10	12.3	CNPRC	SIVmac251	Anti-α4	-
	36798	F	16.11	10.8	CNPRC	SIVmac251	Anti-α4	-
	34051	F	20.00	7.31	CNPRC	SIVmac251	Anti-α4	-
Chronic 251 Cohort (n=6)	38889[&]	F	14.06	11.31	CNPRC	SIVmac251	-	FTC/TDF/DTG
	38919	F	14.06	8.63	CNPRC	SIVmac251	-	FTC/TDF/DTG
	36056	F	18.06	9.96	CNPRC	SIVmac251	-	FTC/TDF/DTG
	37274	F	16.06	8.67	CNPRC	SIVmac251	-	FTC/TDF/DTG
	39359	M	14.04	13.36	CNPRC	SIVmac251	-	FTC/TDF/DTG
	36511[&]	F	17.06	10.34	CNPRC	SIVmac251	-	FTC/TDF/DTG
Control Cohort 1 (n=4)	38163	F	15.07	7.48	CNPRC	-	-	-
	40691	M	12.07	12.18	CNPRC	-	-	-
	38691	F	14.10	13.56	CNPRC	-	-	-
	40499	F	12.11	9.79	CNPRC	-	-	-

Animals in the α4 blockade cohort were included throughout the study and are presented in Figures 1 through 6. Data from control cohort are shown in single-cell analysis, microscopy, and phenotype characterization in Figures 2, 5, and 6. Data from the chronic 251 cohort are shown specifically in Figure 6. SIV: Simian Immunodeficiency Virus; ART: Anti-Retroviral Therapy; FTC: Emtricitabine; TDF: Tenofovir disoproxil fumarate; DTG: Dolutegravir; CNPRC: California National Primate Research Center

*Antibody treatments were administered at 1 week prior to SIV infection and every subsequent 10-day interval at doses of 25mg/kg intravenously over the course of the study.

S2 Table. Details of mice

Strain	Age (Months)	Sex	Date assessed	Blood	Spleen	Liver	PP	Brain	Dura	Sk BM	PBS	LPS
WT-MS-1	6 mo	M	Jan 23 2025	✓	✓	✓	✓	✓	X	X	X	X
WT-MS-2	6 mo	M	Jan 23 2025	✓	✓	✓	✓	✓	X	X	X	X
WT-MS-3	6 mo	M	Jan 23 2025	✓	✓	✓	✓	✓	X	X	X	X
A4 Fl-MS-1	6 mo	M	Jan 23 2025	✓	✓	✓	✓	✓	X	X	X	X
A4 Fl-MS-2	6 mo	M	Jan 23 2025	✓	✓	✓	✓	✓	X	X	X	X
A4 Fl-MS-3	6 mo	M	Jan 23 2025	✓	✓	✓	✓	✓	X	X	X	X
CD4CreA4 Fl-MS-1	6 mo	M	Jan 23 2025	✓	✓	✓	✓	✓	X	X	X	X
CD4CreA4 Fl-MS-2	6 mo	M	Jan 23 2025	✓	✓	✓	✓	✓	X	X	X	X
CD8CreA4 Fl-MS-1	6 mo	M	Jan 23 2025	✓	✓	✓	✓	✓	X	X	X	X
CD8CreA4 Fl-MS-2	6 mo	M	Jan 23 2025	✓	✓	✓	✓	✓	X	X	X	X
CD8CreA4 Fl-MS-3	6 mo	M	Jan 23 2025	✓	✓	✓	✓	✓	X	X	X	X
WT-MS-1	7 mo	F	Feb 27 2025	X	✓	✓	✓	✓	X	X	X	X
WT-MS-2	7 mo	F	Feb 27 2025	X	✓	✓	✓	✓	X	X	X	X
WT-MS-3	7 mo	F	Feb 27 2025	X	✓	✓	✓	✓	X	X	X	X
A4 Fl-MS-1	7 mo	F	Feb 27 2025	X	✓	✓	✓	✓	X	X	X	X
A4 Fl-MS-2	7 mo	F	Feb 27 2025	X	✓	✓	✓	✓	X	X	X	X
CD4CreA4 Fl-MS-1	7 mo	F	Feb 27 2025	X	✓	✓	✓	✓	X	X	X	X
CD8CreA4 Fl-MS-1	7 mo	F	Feb 27 2025	X	✓	✓	✓	✓	X	X	X	X
CD8CreA4 Fl-MS-2	7 mo	F	Feb 27 2025	X	✓	✓	✓	✓	X	X	X	X
A4 Fl-MS-1	3 mo	F	May 22 2025	✓	X	X	X	X	X	X	X	X
A4 Fl-MS-2	3 mo	F	May 22 2025	✓	X	X	X	X	X	X	X	X
A4 Fl-MS-3	3 mo	F	May 22 2025	✓	X	X	X	X	X	X	X	X
A4 Fl-MS-1	3 mo	M	May 22 2025	✓	X	X	X	X	X	X	X	X
A4 Fl-MS-2	3 mo	M	May 22 2025	✓	X	X	X	X	X	X	X	X
CD4CreA4 Fl-MS-1	3 mo	F	May 22 2025	✓	X	X	X	X	X	X	X	X
CD4CreA4 Fl-MS-2	3 mo	F	May 22 2025	✓	X	X	X	X	X	X	X	X
CD4CreA4 Fl-MS-3	3 mo	F	May 22 2025	✓	X	X	X	X	X	X	X	X
CD4CreA4 Fl-MS-1	3 mo	M	May 22 2025	✓	X	X	X	X	X	X	X	X
CD4CreA4 Fl-MS-2	3 mo	M	May 22 2025	✓	X	X	X	X	X	X	X	X
CD4CreA4 Fl-MS-3	3 mo	M	May 22 2025	✓	X	X	X	X	X	X	X	X
CD4CreA4 Fl-MS-1	3-4 mo	F	April 20 2025	✓	✓	✓	✓	✓	✓	✓	X	✓
CD8CreA4 Fl-MS-1	3-4 mo	F	April 20 2025	✓	✓	✓	✓	✓	✓	✓	X	✓
CD8CreA4 Fl-MS-2	3-4 mo	F	April 20 2025	✓	✓	✓	✓	✓	✓	✓	X	✓
A4 Fl-MS-1	3-4 mo	F	April 20 2025	✓	✓	✓	✓	✓	✓	✓	X	✓
A4 Fl-MS-2	3-4 mo	F	April 20 2025	✓	✓	✓	✓	✓	✓	✓	X	✓
A4 Fl-MS-3	3-4 mo	F	April 20 2025	✓	✓	✓	✓	✓	✓	✓	X	✓
A4 Fl-MS-1	4 mo	F	Jun 20 2025	✓	✓	✓	✓	✓	✓	✓	✓	X
A4 Fl-MS-2	4 mo	F	Jun 20 2025	✓	✓	✓	✓	✓	✓	✓	✓	X
CD4CreA4 Fl-MS-1	4 mo	F	Jun 20 2025	✓	✓	✓	✓	✓	✓	✓	✓	X
CD4CreA4 Fl-MS-2	4 mo	F	Jun 20 2025	✓	✓	✓	✓	✓	✓	✓	✓	X
A4 Fl-MS-1	4 mo	F	Jun 20 2025	✓	✓	✓	✓	✓	✓	✓	X	✓
A4 Fl-MS-2	4 mo	F	Jun 20 2025	✓	✓	✓	✓	✓	✓	✓	X	✓
CD4CreA4 Fl-MS-1	4 mo	F	Jun 20 2025	✓	✓	✓	✓	✓	✓	✓	X	✓
CD4CreA4 Fl-MS-2	4 mo	F	Jun 20 2025	✓	✓	✓	✓	✓	✓	✓	X	✓
A4 Fl-MS-1	4 mo	F	July 3 2025	✓	✓	✓	✓	✓	✓	✓	✓	✓
CD4CreA4 Fl-MS-1	4 mo	F	July 3 2025	✓	✓	✓	✓	✓	✓	✓	✓	✓
A4 Fl-MS-1	4 mo	F	July 3 2025	✓	✓	✓	✓	✓	✓	✓	X	✓
A4 Fl-MS-2	4 mo	F	July 3 2025	✓	✓	✓	✓	✓	✓	✓	X	✓
A4 Fl-MS-3	4 mo	F	July 3 2025	✓	✓	✓	✓	✓	✓	✓	X	✓
CD4CreA4 Fl-MS-1	4 mo	F	July 3 2025	✓	✓	✓	✓	✓	✓	✓	X	✓
CD4CreA4 Fl-MS-2	4 mo	F	July 3 2025	✓	✓	✓	✓	✓	✓	✓	X	✓
CD4CreA4 Fl-MS-3	4 mo	F	July 3 2025	✓	✓	✓	✓	✓	✓	✓	X	✓
CD8CreA4 Fl-MS-1	4 mo	M	July 14 2025	✓	X	X	X	X	X	X	X	X
CD8CreA4 Fl-MS-2	4 mo	M	July 14 2025	✓	X	X	X	X	X	X	X	X
CD8CreA4 Fl-MS-3	4 mo	M	July 14 2025	✓	X	X	X	X	X	X	X	X
CD8CreA4 Fl-MS-4	4 mo	M	July 14 2025	✓	X	X	X	X	X	X	X	X
CD8CreA4 Fl-MS-5	4 mo	M	July 14 2025	✓	X	X	X	X	X	X	X	X
CD8CreA4 Fl-MS-6	4 mo	M	July 14 2025	✓	X	X	X	X	X	X	X	X
A4 Fl-MS-1	4 mo	M	July 14 2025	✓	X	X	X	X	X	X	X	X
A4 Fl-MS-2	4 mo	M	July 14 2025	✓	X	X	X	X	X	X	X	X
A4 Fl-MS-3	4 mo	M	July 14 2025	✓	X	X	X	X	X	X	X	X
A4 Fl-MS-4	4 mo	M	July 14 2025	✓	X	X	X	X	X	X	X	X
A4 Fl-MS-1	4 mo	F	July 17 2025	✓	✓	X	X	✓	✓	✓	X	✓
A4 Fl-MS-2	4 mo	F	July 17 2025	✓	✓	X	X	✓	✓	✓	X	✓
A4 Fl-MS-3	4 mo	F	July 17 2025	✓	✓	X	X	✓	✓	✓	X	✓
CD8CreA4 Fl-MS-1	4 mo	F	July 17 2025	✓	✓	X	X	✓	✓	✓	X	✓
CD8CreA4 Fl-MS-2	4 mo	F	July 17 2025	✓	✓	X	X	✓	✓	✓	X	✓
CD8CreA4 Fl-MS-3	4 mo	F	July 17 2025	✓	✓	X	X	✓	✓	✓	X	✓
CD8CreA4 Fl-MS-4	4 mo	F	July 17 2025	✓	✓	X	X	✓	✓	✓	X	✓
CD8CreA4 Fl-MS-5	4 mo	F	July 17 2025	✓	✓	X	X	✓	✓	✓	X	✓

Supplementary Table 2. Details of mice. Summary of mouse strains, ages, sexes, tissues collected, and treatment assignments. Checkmarks indicate tissues collected and analyzed; X indicates tissues not collected. PBS and LPS columns indicate treatment group assignment. WT, wild-type; A4 Fl, *Itga4*^fl/fl^; CD4CreA4 Fl, CD4-Cre *Itga4*^fl/fl^ (CD4^Δ*Itga4*^); CD8CreA4 Fl, CD8-Cre *Itga4*^fl/fl^ (CD8^Δ*Itga4*^); MS, mouse; mo, months; PP, Peyer's patches; Sk BM, skull bone marrow; PBS, phosphate-buffered saline; LPS, lipopolysaccharide.

S3 Table. Antibody reagents for Flow Cytometry Analysis.

S. No	Reagents	Source	Catalog number
1.	AF700 anti-human CD3 (Clone SP34-2)	BD Biosciences	Cat#557917
2.	APC-Cy7 anti-human CD3 (Clone SP34-2)	BD Biosciences	Cat#557757
3.	BV650 anti-human CD4 (Clone L200)	BD Biosciences	Cat#563737
4.	BUV805 anti-human CD8 (Clone SK1)	BD Biosciences	Cat#612889
5.	BUV737 anti-human CD95 (Clone DX2)	BD Biosciences	Cat#564710
6.	PE/Dazzle 594 anti-human CD28 (Clone CD28.2)	BioLegend	Cat#302942
7.	APC-Cy7 anti-human CD20 (Clone 2H7)	BioLegend	Cat#302314
8.	APC-Cy7 anti-human live/dead	invitrogen	Ref#L34976A
9.	PE anti-human CD197 (CCR7) (Clone 3D12)	BD Biosciences	Cat#561008
10.	BV785 anti-human CD195 (CCR5) (Clone 3A9)	BD Biosciences	Cat#565001
11.	PE-CF594 Mouse Anti-Human CD196 (CCR6) (Clone 11A9)	BD Biosciences	Cat#564816
12.	BV711 anti-human CD69 (Clone FN50)	BioLegend	Cat#310944
13.	FITC anti-human CD49d (Clone HP2/1)	Beckman Coulter	Part no#IM1404U
14.	PE/Dazzle™ 594 anti-human/mouse Integrin β7 (Clone FIB504)	BioLegend	Cat#321226
15.	PE anti-human Integrin β1 (Clone TS2/16)	BioLegend	Cat#303003
16.	APC anti-human CD183 (CXCR3) (1C6/CXCR3)	BD Biosciences	Cat#550967
17.	PECy7 anti-human PD1 (Clone EH12.2H8)	BioLegend	Cat#329918
18.	FITC anti-human TNF-α (Clone Mab11)	BioLegend	Cat#502906
19.	PECy7 anti-human IFNγ (Clone B27)	BioLegend	Cat#506518
20.	PE/Dazzle™ 594 anti-human IL-2 (Clone MO1-17H12)	BioLegend	Cat#500344
21.	BUV395 anti-mouse Ki67 (Clone B56)	BD Biosciences	Cat#564071
22.	BUV563 anti-mouse CXCR3 (Clone CXCR3-173)	BD Biosciences	Cat#741438
23.	BUV661 anti-mouse CD3 (Clone 17A2)	BD Biosciences	Cat#741562
24.	BUV737 anti-mouse CD44 (Clone IM7)	BD Biosciences	Cat#612799
25.	BUV805 anti-mouse CD8a (Clone 53-6.7)	BD Biosciences	Cat#612898
26.	BV605 anti-mouse CD11b (Clone M1/70)	BD Biosciences	Cat#563015
27.	BV650 anti-mouse CD4 (Clone RM4-5)	BD Biosciences	Cat#563747
28.	BV711 anti-mouse CD162 (Clone 2PH1)	BD Biosciences	Cat#740746
29.	BV785 anti-mouse CD45 (Clone 30-F11)	Biolegend	Cat#103149
30.	PerCP/Cy5.5 anti-mouse CD11a/CD18 (LFA-1) (Clone H155-78)	Biolegend	Cat#141008
31.	PerCP-eFlour™710 anti-mouse Int β1 CD29 (Clone HMb1-1)	Invitrogen	Cat#46-0291-82
32.	PE/Dazzle™ 594 anti-mouse CD49d (Clone R 1-2)	BioLegend	Cat#103626
33.	PE-Cy5 anti-mouse FOXP3 (Clone FJK-16s)	Invitrogen	Cat#15-5773-82
34.	PE/Cy7 anti-mouse CD279 (PD-1) (Clone RMP1-30)	BioLegend	Cat#109110
35.	FACS lyse	BD Biosciences	Cat#349202
36.	FoxP3/ Transcription Factor Staining Buffer set	invitrogen	Cat#00-5523
37.	Brilliant stain buffer	BD Biosciences	Cat#563794

CD: cluster of differentiation; PE: Phycoerythrin; AF: Alexa Fluor; BV: Brilliant violet; BUV: Brilliant ultraviolet; Cy: Cyanine; APC: Allophycocyanin; FITC: Fluorescein Isothiocyanate conjugated